PSEUDODYNAMIC TEST OF SEISMIC ISOLATOR PROTOTYPE WITH U-SHAPED DAMPERS

ENSAYO PSEUDODINÁMICO DE UN PROTOTIPO DE AISLADOR SÍSMICO CON DISIPADORES EN FORMA DE "U"

Luis Nuñez[1*], Carlos Zavala[1,2], Roy Reyna[1,2]

[1] *Japan-Peru Center for Earthquake Engineering Research and Disaster Mitigation, National University of Engineering, Lima, Peru*

[2] *Faculty of Civil Engineering, National University of Engineering, Lima, Peru*

Received (Recibido): 26 / 02 / 2025 Publicado (Published): 30 / 12 / 2025

ABSTRACT

The pseudodynamic testing technique combines numerical step-by-step integration with an experimental displacement-based control system to explore the seismic response of structures. Although this method has undergone significant development and has proven to be reliable and effective, its implementation in structural laboratories across Peru remains limited. To help bridge this gap, the present study applies a conventional pseudodynamic test using the control, loading, and data acquisition systems available at the Laboratory of Structures of the Japan-Peru Center for Earthquake Engineering Research and Disaster Mitigation (CISMID). The aim is to assess the performance of the control algorithm through two tests conducted on a seismic isolator prototype that incorporates U-shaped dampers. The specimen is loaded axially to simulate the tributary area of a two-story structure and is subjected to two levels of seismic input derived from the 1974 Lima earthquake record. A comparative analysis is carried out between experimental and numerical responses. The findings reveal effective displacement control and a reasonable correlation between experimental data and numerical simulations.

Keywords: Pseudodynamic test, On-line control, Experimental technique, Control algorithm, Seismic Isolator.

RESUMEN

La técnica de ensayo pseudodinámico combina la integración numérica paso a paso con un sistema experimental de control basado en desplazamientos para explorar la respuesta sísmica de las estructuras. Aunque este método ha experimentado un desarrollo significativo y ha demostrado ser confiable y eficaz, su implementación en los laboratorios estructurales del Perú sigue siendo limitada. Con el fin de ayudar a reducir esta brecha, el presente estudio aplica un ensayo pseudodinámico convencional utilizando los sistemas de control, carga y adquisición de datos disponibles en el Laboratorio de Estructuras del Centro Peruano-Japonés de Investigaciones Sísmicas y Mitigación de Desastres (CISMID). El objetivo es evaluar el desempeño del algoritmo de control a través de dos ensayos realizados sobre un prototipo de aislador sísmico que incorpora amortiguadores en forma de U. El espécimen se carga axialmente para simular el área tributaria de una estructura de dos pisos y se somete a dos niveles de entrada sísmica derivados del registro del sismo de Lima de 1974. Se realiza un análisis comparativo entre las respuestas experimentales y numéricas. Los resultados revelan un control efectivo del desplazamiento y una correlación razonable entre los datos experimentales y las simulaciones numéricas.

Palabras Clave: Ensayo pseudodinámico, control en-línea, Técnica experimental, Algoritmo de control, Aislador sísmico.

1. INTRODUCTION

Recently, structural testing techniques have been implemented, developed and applied for the experimental seismic evaluation of structures in laboratories. Among these techniques, pseudodynamic testing (PSD) method has gained importance as a fundamental testing tool for assessing the seismic behavior of structures. This method enables the on-line simulation of displacements and forces generated by seismic excitation that might impact structures in real-life scenarios, offering advantages in terms of load capacity, cost, and infrastructure requirements compared to other techniques, such as shaking table tests [1].

[1] * Corresponding author:
E-mail: lnunezn@uni.pe

PSD testing applications have become increasingly common in laboratories around the world. One of the most relevant PSD implementations was carried out at the University of Toronto where a cross-platform program interface was developed for numerical-experimental simulations (e.g. real-time PSD tests). This program integrates modules for numerical integration, substructure analysis, actuator control, data exchange, and numerical error compensation [2]. Another application of real-time PSD simulation was conducted at the Indian Institute of Technology Kanpur. In this institute, the PSD technique was applied to a two-story reinforced concrete frame equipped with a viscoelastic damper [3]. Similarly, this experimental technique was implemented at the University of Napoli Federico II to understand the interaction between a non-structural brick wall and a reinforced concrete frame during a seismic event, focusing on structures common in the Mediterranean region [4].

Advancements in control technology have significantly improved the efficiency and capabilities of PSD tests, expanding its applications. For instance, PSD tests have been developed to evaluate of large-scale substructures, such as a two-story steel frame system within a complete structure [5]. In addition, the method has been employed to investigate the experimental behavior of an elastomeric seismic isolator substructure, with the superstructure simulated numerically [6]. Despite the considerable potential of PSD technique, its application remains uncommon in structural laboratories in Peru. This might be attributed to challenges related to compatibility with current control system devices, as well as the complexity of implementation and the specialized training required for operators, technicians, and support staff.

To address this gap, this research aims to apply a PSD testing technique using the facilities of the Structural Laboratory at the Japan-Peru Center for Earthquake Engineering Research and Disaster Mitigation (CISMID). For this purpose, a displacement control algorithm is employed to ensure accurate tracking of the target displacement. To validate the effectiveness of this algorithm, two PSD tests are conducted on a seismic isolator specimen equipped with U-shaped steel dampers. Additionally, the parameters of bilinear hysteresis model are calibrated using experimental data. Finally, a comparative analysis is carried out between the experimental results and a numerical simulation. The findings demonstrate an effective displacement control and a reasonable correlation between the experimental and numerical responses.

2. METHODOLOGY

2.1. CISMID Laboratory Facilities

The Structural Laboratory of CISMID has contributed extensively to the development of seismic research through experimental tests that evaluate structural performance under static and dynamic loads. This laboratory is equipped with a large reaction wall and devices (e.g., servo-hydraulic actuators, shaking table, sensors, data acquisition system, etc.) that enable the safe and reliable execution of tests on full-scale specimens and scaled models.

In the context of this investigation, Shimadzu servo-hydraulic actuators and a data acquisition system are utilized to execute the pseudodynamic tests. The actuators feature a maximum load capacity of ±75 tonf, a stroke of ±200 mm, and a loading speed of 2 mm/s. The actuator's motion is precisely controlled by its servo-valve, which operates through a servo-controller that allows the user to configure the desired displacement. Fig. 1 shows the actuator-controller system from the CISMID Structural Laboratory, consisting primarily of Shimadzu actuators and Servo-controllers.

(a) (b)

Fig. 1. The CISMID's Laboratory Actuator system: (a) Servo-hydraulic actuator, (b) Servo-controller.

The data acquisition system consists of linear variable differential transformers (LVDTs), a 16-bit USB-6003 analog-to-digital converter with a sampling rate of up to 100 kS/s, and a custom-developed software implemented in LabVIEW2020 platform using visual programming language. These components are illustrated in Fig. 2 and provide the laboratory with precise and reliable tools for executing large experimental techniques such as pseudodynamic testing.

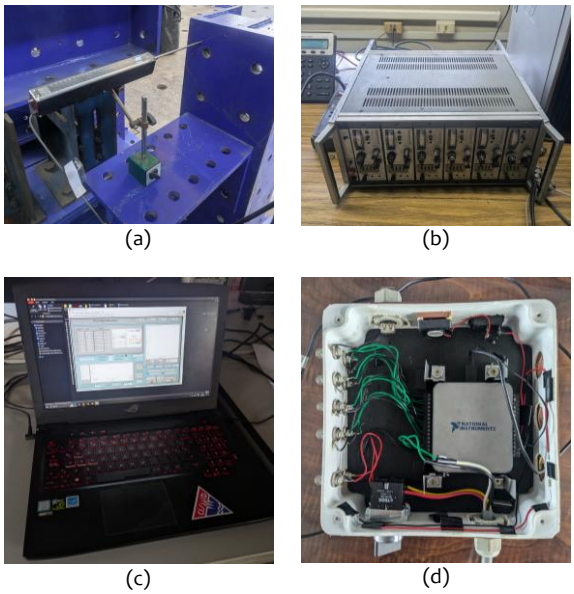

(a) (b) (c) (d)

Fig. 2. Equipment in the control cabinet: (a) LVDT, (b) Data acquisition, (c) Computer, (d) USB-6003.

2.2. Pseudodynamic (PSD) Test Framework

The PSD is an experimental technique in which controlled displacements are applied to a structure to simulate its response under seismic excitation. Instead of directly imposing seismic loads on the base of the specimen (e.g. shaking table testing), the PSD technique employs actuators for replicating the displacement response of the structure, which is mathematically calculated by a computer [7].

In Peru, the first PSD test was implemented in the C programming language by Scaletti et. al. in 1992 at the CISMID Structural Laboratory, leading to several subsequent application studies [8], [9]. Later, Chunga developed an updated software for conducting PSD tests using visual programming language and a graphical interface on a Windows 98 computer [10]. However, this program is no longer compatible with current operating system and control technologies.

In PSD tests, the response is obtained by modeling the structure as a mechanical system and solving its behavior through a numerical integration method. In this research, the explicit Newmark method was chosen for the PSD integration process due to its suitability for conventional testing procedures [11]. Equation (1) represents the equation of motion that governs the dynamic of a specimen idealized as a single-degree-of-freedom (SDOF) system, as shown below:

$$m\ddot{x}_i + c\dot{x}_i + kx_i = -m\ddot{x}_{g,i} \qquad (1)$$

where m, k, c are the mass, stiffness and damping coefficient of the specimen, respectively. Moreover, x_i, $\dot{x}_i$, $\ddot{x}_i$ represent the response in displacement, velocity and acceleration at the step i subject to a ground excitation $\ddot{x}_g$. Then, equations of the Newmark method are presented as follows:

$$x_{i+1} = x_i + \Delta t\dot{x}_i + \frac{\Delta t^2}{2}\ddot{x}_i \qquad (2)$$

$$\bar{m}\ddot{x}_{i+1} = -m\ddot{x}_{g,i+1} - f_{r,i+1} - c\dot{x}_i - \frac{\Delta t}{2}c\ddot{x}_i \qquad (3)$$

$$\bar{m} = m + \frac{\Delta t}{2}c \qquad (4)$$

$$\dot{x}_{i+1} = \dot{x}_i + \frac{\Delta t}{2}(\ddot{x}_i + \ddot{x}_{i+1}) \qquad (5)$$

where $f_{r,i+1}$ is the restoring force at the step $i+1$, and Δt is the time step for the numeric integration process. To ensure the stability, it is required that the time step satisfies the stability condition $\Delta t \leq \frac{T}{\pi}$, where T is the natural period of the system.

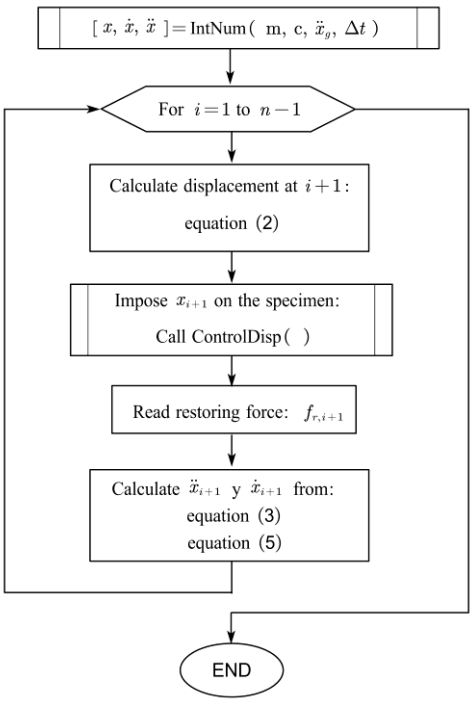

Fig. 3. Flowchart of the Explicit Newmark method in PSD.

Fig. 3 illustrates the direct integration routine (labeled as *IntNum*) into the pseudodynamic testing process. The mass and damping coefficient are considered as simulation input data. The target displacement is imposed on the specimen under a displacement control (*ControlDisp*) that is discussed later in Section 2.3. Once the desired displacement is achieved, the restoring force is measured on-line

using internal load cells installed within the actuator. This restoring force is used to calculate the displacement at the next step in the numerical integration loop. This process is carried out for each time-step during the time domain.

To apply the online technique, the computer calculates the displacement desired (digital), which is converted into a corresponding analog voltage signal by means of the USB-6003 converter and transmitted to the servo-controller. The servo-controller processes this signal and sends it to the servo-valve, which regulates the actuator's motion. Physical measurements, such as displacements and forces, are recorded and sent back to the computer (feedback process) to enable displacement control and calculate the response at the next step. A schematic representation of this hybrid procedure is shown in Fig. 4, where the PSD simulation interacts with the physical test setup. Thus, the actuator piston displacement (stroke), the restoring load, and the specimen's deformation are monitored and recorded on real-time through the servo-controller feedback and sensors placed on the specimen. This ensures a seamless integration between the hardware and the control algorithm.

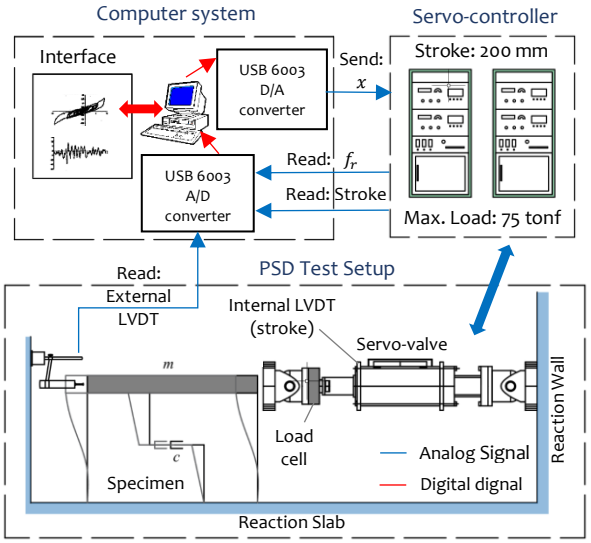

Fig. 4. Hardware-software interaction Scheme in a PSD test at CISMID.

2.3. Control Algorithm

The equivalent voltage corresponding to the target displacement is initially sent to the actuator-controller system. However, due to the specimen's stiffness, the target displacement might not be achieved initially, resulting in an error between the desired value and the one measured by the specimen's deformation sensor [12]. To address this issue, a displacement control algorithm (labeled as *ControlDisp*) is employed.

The core principles of the control algorithm procedure over two consecutive time steps are schematized in Fig. 5. It is assumed that the target displacement is achieved in j cycles for both time steps. Let $e_{m.i}^{(j)}$ be the error at step i between the target displacement x_i and the measured deformation $x_{m.i}^{(j)}$ at cycle j. This procedure involves sending additional monotonic voltage signals ΔV until the error is reduced below a predefined tolerance ε of 0.01 V. This voltage increment is adjusted based on the error $e_{m.i}^{(j)}$ as expressed below:

$$\Delta V = 0.5 \sum_{p=1}^{j} e_{m,i}^{(p)} \qquad (6)$$

This criterion ensures the monotonic actuator action. This must be satisfied because an unloading in the control process could lead to a deterioration of the specimen's stiffness that does not represent its seismic behavior [13].

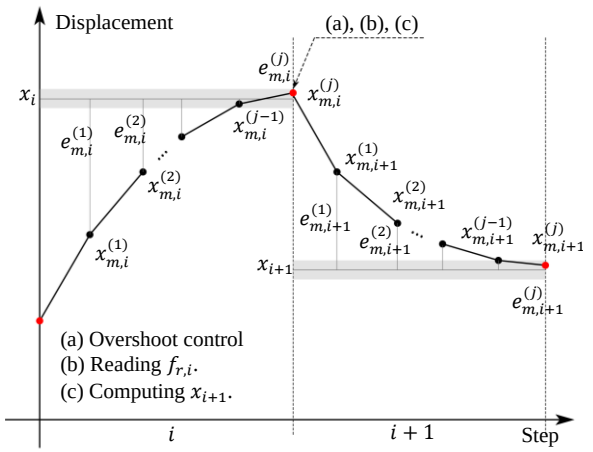

Fig. 5. Displacement control scheme in PSD.

Once the control convergence cycle is completed, the measured deformation is not strictly the same as the computed displacement since the finite resolution of sensors. Therefore, the measured deformation might either be below (undershoot) or above (overshoot) the target displacement within the predefined tolerance. In this research an overshoot condition is chosen for displacement control of the PSD test [10], [13]. Therefore, the control criteria are summarized in the following expression:

$$\left(x_{m,i+1}^{(j)} - x_{m,i+1}^{(j-1)}\right)\left(x_{t,i+1} - x_{m,i+1}^{(j)}\right) \geq 0 \qquad (7)$$

This control strategy is shown in the flowchart presented in Fig. 6. Moreover, a delay time of 500ms is included to allow the actuator piston to respond to the signal sent.

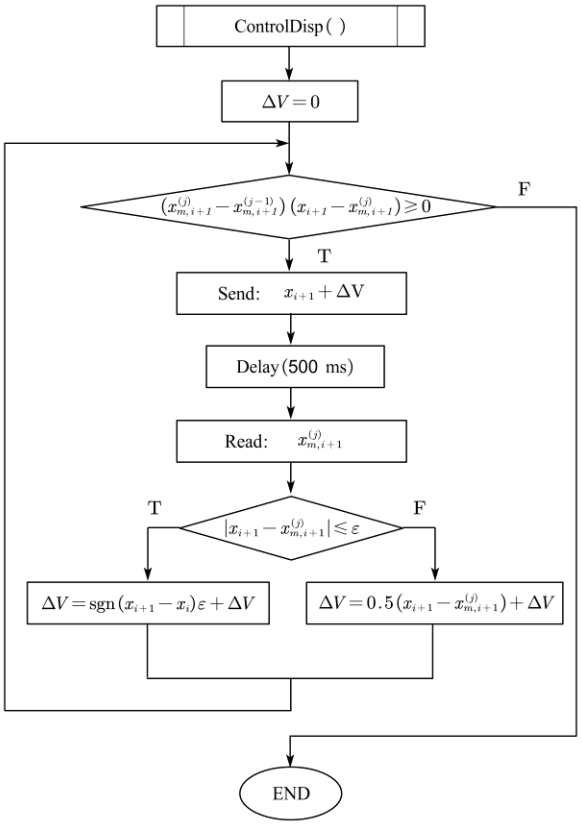

Fig. 6. Flowchart of the displacement control in PSD [13].

3. EXPERIMENTAL STUDY

To evaluate the feasibility and effectiveness of the control algorithm, two PSD tests are conducted on a seismic isolator prototype equipped with U-shaped steel dampers. These tests were performed on the same specimen under two different levels of axial load and ground excitation. The specimen description, test setup, and PSD input are discussed in this section.

3.1. Specimen description

The specimen, (labeled as ABC-RU), is an elastomeric seismic isolator prototype equipped with U-shaped steel dampers. The ABC-RU specimen was manufactured as part of the FIC-FI-13-2020 project in 2020 [14]. This project was funded by the National University of Engineering (UNI) and led to the research conducted by Reyna et al. in 2024 [15]. In this reference, the specimen was tested under cyclic forces with controlled displacements following the procedure outlined in the Peruvian standard NTP E.031 "Seismic Isolation" [16].

The dimensions of the ABC-RU specimen are depicted in Fig. 7. Its rubber bearing, made from recycled rubber, has a diameter of 300 mm and a height of 150 mm. Inside the bearing, there are 18 steel plates, each with a diameter of 290 mm and a thickness of 2 mm, uniformly distributed along the bearing's height, as shown in Fig. 7 (a). Four U-shaped steel dampers were installed at 45-degree angle from bearing's central axis. The dampers are fabricated from ASTM A36 steel, whose length, width, and thickness are 500 mm, 40 mm, and 19 mm, respectively (see Fig. 7 (b)). The design of this specimen is described in detail in reference [15].

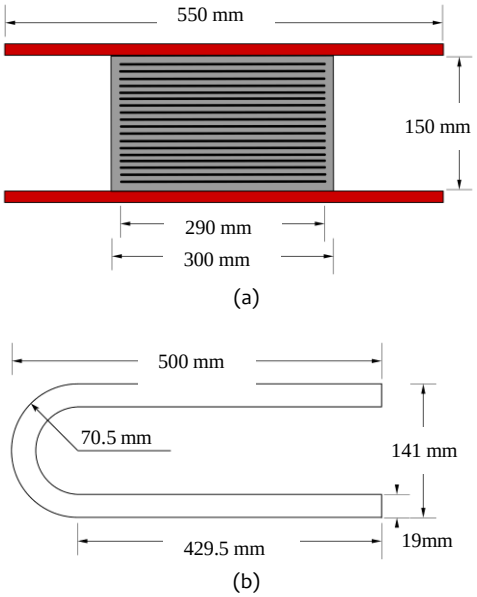

Fig. 7. ABC-RU specimen dimensions: (a) Rubber bearing, (b) U-shaped steel damper [15].

3.2. Test Setup

A test setup similar to the one used in the previous research [15] was assembled for the PSD test execution. This test setup is illustrated in Fig. 8. Two Shimadzu actuators are employed, providing both axial and lateral loads to the specimen.

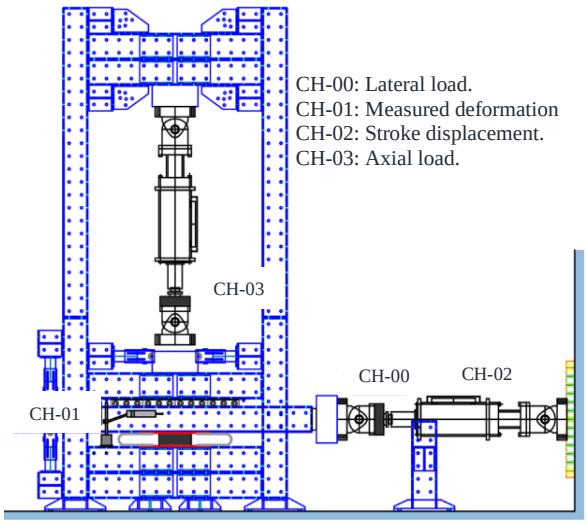

Fig. 8. PSD Test Setup [15].

Additionally, a displacement sensor for specimen deformation is placed on the specimen. Thus, four measurement channels (CH-00, CH-01, CH-02, and CH-03) are configured. These channels correspond to the lateral load, the measured specimen deformation, the actuator's piston displacement (stroke displacement), and the axial load, respectively.

3.3. PSD Testing Input

Two PSD tests (PSD1 and PSD2) were carried out on the same specimen under two levels of axial load and ground excitation. The axial loads were configured at 8.90 tonf and 19.50 tonf by the vertical actuator at the beginning of the PSD tests. These axial loads correspond to those used in the previous research work [15], which represent the average and maximum axial load combinations as specified by the Peruvian standard NTP E0.31 [16] for its associated tributary area. This tributary area is covered by an ABC-RU prototype within a 14-isolator system for a benchmark two-story masonry structure [17], as depicted in Fig. 9.

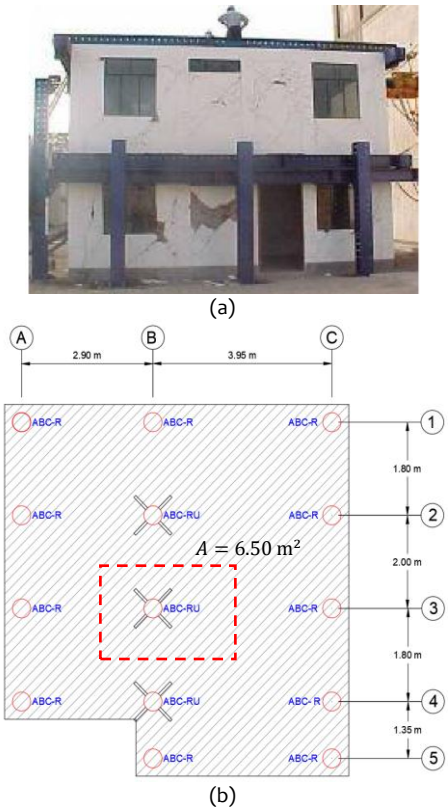

Fig. 9. Benchmark building [17]: (a) Photography, (b) Plan view of isolation system [15].

The ground excitation inputs for the PSD1 and PSD2 tests are shown in Fig. 10. These records were derived from 15 critical seconds of the 1974 Lima earthquake record. To stablish the two levels of ground motion excitation, the record was spectrally scaled to match two design spectra corresponding to return periods of 475 and 2500 years using the natural period T [16], [18]. Additionally, the natural period T and critical damping ratio ζ were adopted from previous studies [14], [15]. The critical damping ratio of 5% corresponds to linear viscous damping obtained from free vibrations tests and does not reflect hysteresis damping, which arises during inelastic pseudodinamic response. All these parameters are summarized in Table I and are used as data input for the PSD tests.

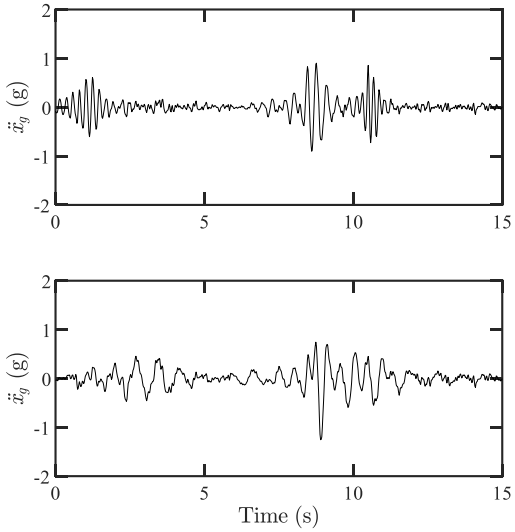

Fig. 10. Ground motion input: (a) PSD1, (b) PSD2.

TABLE I
Pseudodynamic test parameters

Test	Axial Load, f_a (tonf)	Ground excitation PGA (g)	Period, T (s)	Critical Damping ratio, ζ
PSD1	8.90	0.90	0.183	0.05
PSD2	19.50	1.25	0.261	0.05

4. PSD TEST RESULTS

In this section, PSD test results are presented and discussed. Fig. 11 shows the axial force time history during the PSD1 and PSD2 tests. It is observed that the axial forces exhibit variations, with respect to the values mentioned earlier in Section 3.3, due to the unloading of the reaction force when large specimen's deformation are achieved.

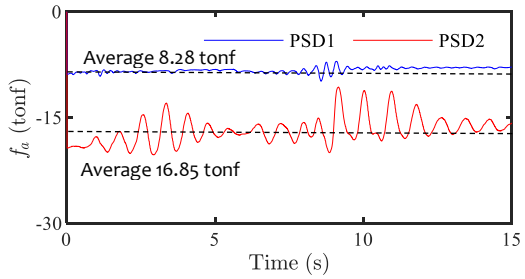

Fig. 11. Time-story of axial load for PSD1 and PSD2.

The time-history of target displacement x and the measured deformation x_m are compared to assess the reliability of the control algorithm, as depicted in Fig. 12. These two variables are evaluated in terms of the root mean square (RMS) and maximum (MAX) responses, obtaining the values shown in Table II. The RMS response differs by no more than 0.15% for both tests, while the maximum response errors are 0.16% and 0.27% for the PSD1 and PSD2 tests, respectively.

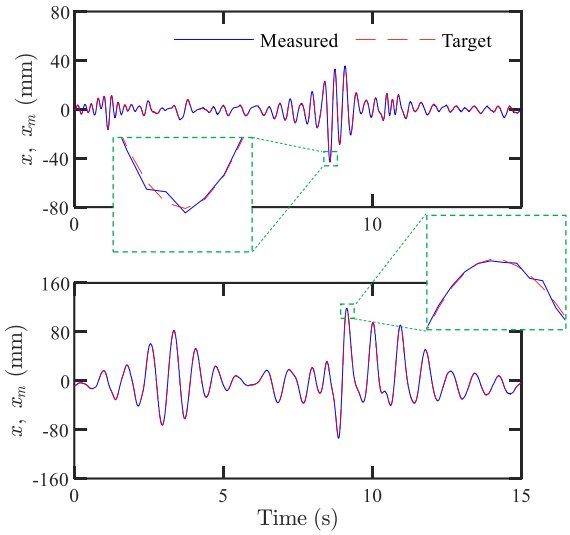

Fig. 12. Time-history of calculated and measured specimen deformation: (a) PSD1, (b) PSD2.

TABLE II
Comparison response between computed displacement and specimen's deformation

	RMS		MAX	
	Measured deformation x_m	Target disp. x_t	Measured deformation x_m	Target disp. x_t
PSD1	7.35	7.34	43.25	42.86
PSD2	31.92	31.87	118.46	118.78

These results demonstrate the effectiveness of the control algorithm using the laboratory equipment at CISMID. Additionally, Fig. 13 presents the time-history of the restoring force. It is noted that maximum lateral load values of 6.05 tonf y 9.79 tonf were achieved during PSD1 and PSD2 tests, respectively.

The hysteresis behavior between specimen's deformation and restoring force during the PSD1 test is illustrated in Fig. 14. The maximum recorded lateral displacement was 43.25 mm, and the peak restoring force reached 6.05 tonf. Additionally, Fig. 15 displays critical instances of maximum deformation of the specimen during the PSD1 test. The maximum tension load of 4.84 tonf is reached at a displacement of 35.44 mm, while under maximum compression load of 6.05 tonf, it reaches a deformation of 43.25 mm.

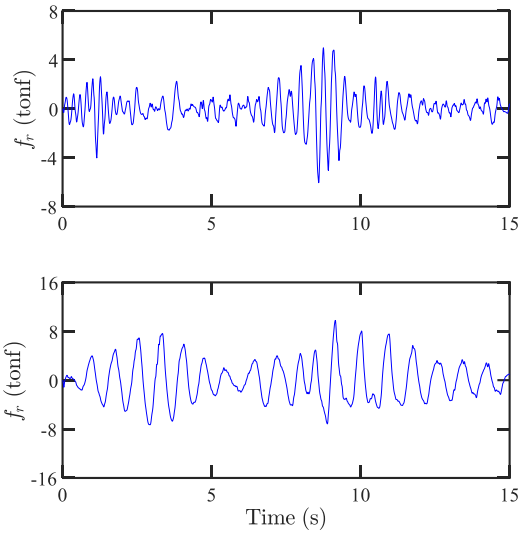

Fig. 13. Time-history of measured restoring force: (a) PSD1, (b) PSD2.

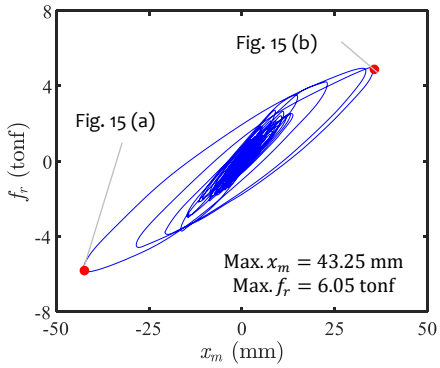

Fig. 14. Hysteresis loop of specimen's deformation against restoring force for PSD1.

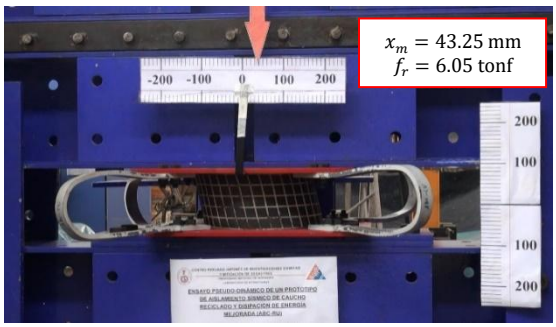

(a)

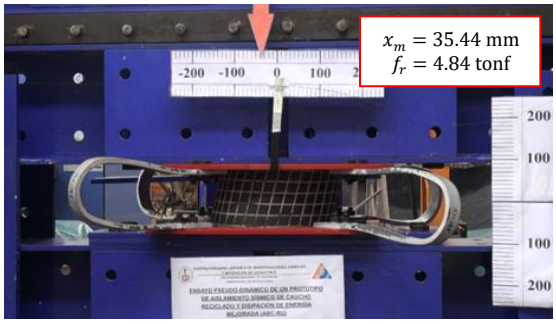

(b)

Fig. 15. Maximum deformation points for PSD1: (a) Compression load, (b) Tension load.

On the other hand, Figure 16 provides the hysteresis curve for the PSD2 test, where the specimen reached a maximum lateral displacement of 118.46 mm for a maximum restoring force of 9.79 tonf. In Figure 17, maximum deformation instances during the PSD2 test are presented as well. At the instant of maximum compression load, the specimen deforms 94.77 mm with a lateral force of 7.67 tonf. Similarly, when the actuator is under a tensile load of 9.79 tonf, the specimen's deformation reaches 118.46 mm.

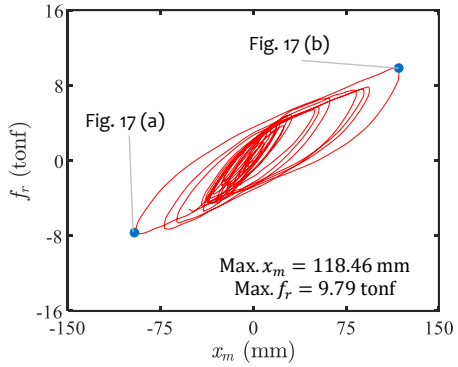

Fig. 16. Hysteresis loop of specimen's deformation against restoring force for PSD2.

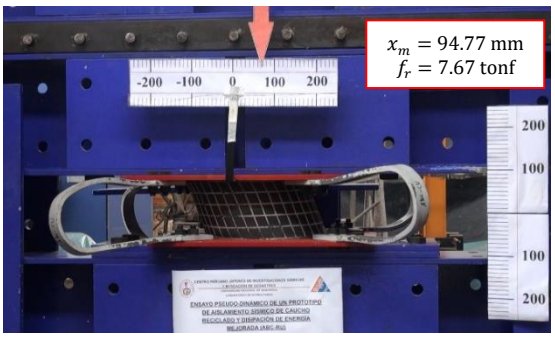

(a)

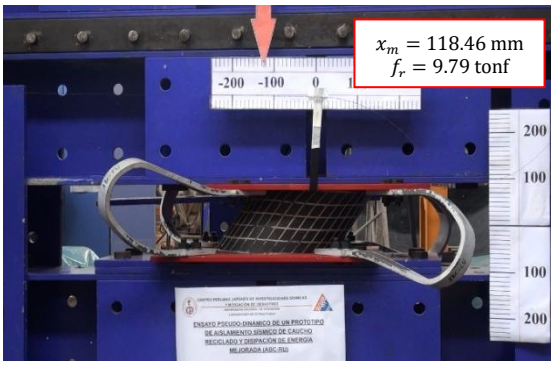

(b)

Fig. 17. Maximum deformation points for PSD2: (a) Actuator pushing, (b) Actuator pulling.

5. NUMERICAL SIMULATION

Numerical simulations of a single-degree-of-freedom (SDOF) system was conducted. These simulations were based on the idealized model of the specimen used in the PSD tests (PSD1 and PSD2). A bilinear hysteresis model was applied to replicate the dynamic behavior observed experimentally. The parameters for the bilinear model are defined in Fig. 18 and obtained by calibrating to the experimental data.

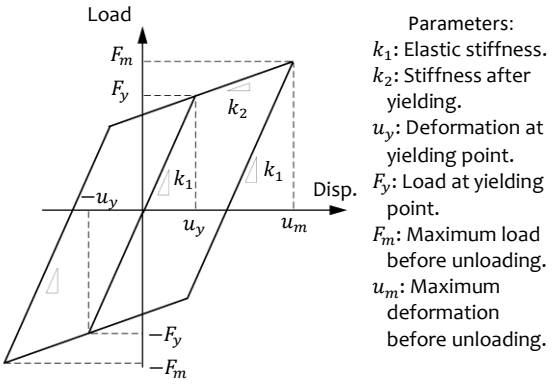

Fig. 18. Bilinear hysteresis model parameters.

The parameters derived from the bilinear hysteresis model for PSD1 and PSD2 tests are shown in Fig. 19. As expected, the elastic stiffness k_1 for PSD2, which involved higher seismic excitation and axial load, is greater than that observed for PSD1. Moreover, the post-yielding stiffness k_2 is lower for PSD2 compared to PSD1. For both tests, the yielding deformation u_y is consistent at 14 mm.

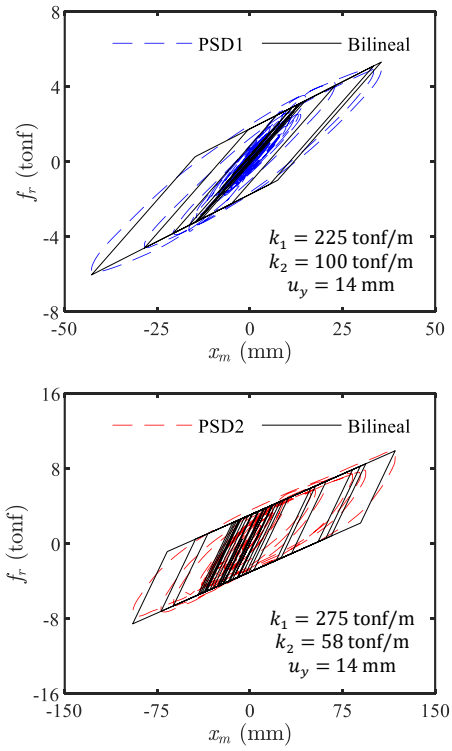

Fig. 19. Equipment in the control cabinet.

Fig. 20 and Fig. 21 illustrates time history responses of displacement and restoring force for PSD1 and PSD2, respectively, where the experimental data is compared to that obtained from numerical simulation. The numerical results reasonably approximate the experimental behavior of the system, capturing the essential characteristics of the specimen's response under seismic excitation. The numerical simulations offer a reasonable representation of the specimen's response.

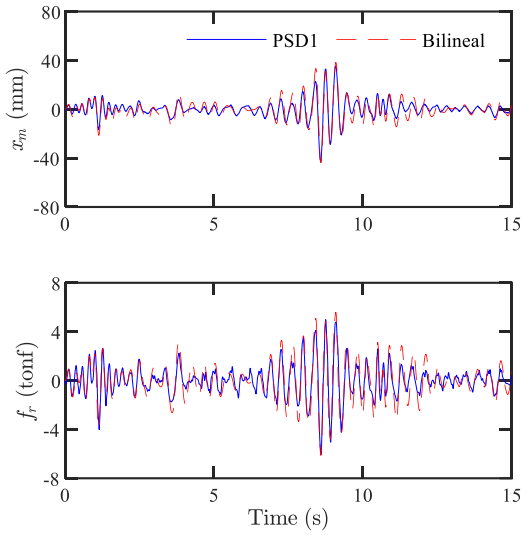

Fig. 20. Time-history comparison responses between experimental data and bilinear model (PSD1).

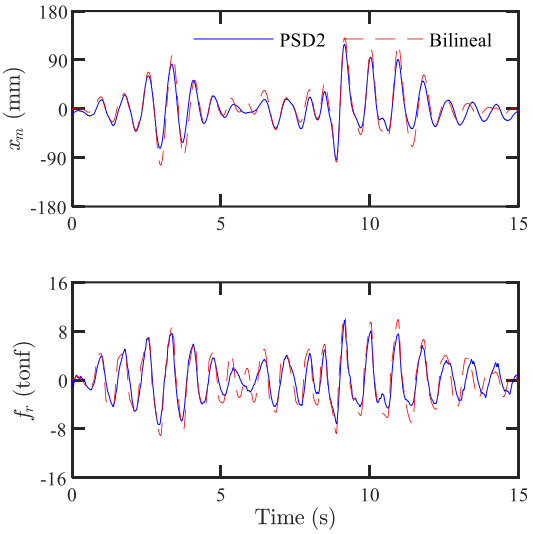

Fig. 21. Time-history comparison responses between experimental data and bilinear model (PSD2).

The results from experimental and numerical simulation are compared in terms of RMS and MAX responses for PSD1 and PSD2. These results are shown in Table III and Table IV, respectively. For the PSD1 test, the RMS error in deformation reached 21%, while the RMS error in restoring force was 26.92%. In addition, errors of MAX response in deformation and restoring force errors were 1.16% and 1.32%, respectively. On the other hand, for the PSD2 test, the RMS errors in deformation and restoring force were 19.96% and 23.93%, respectively. The errors of MAX response were higher compared to PSD1, with 10.21% for deformation and 8.69% for restoring force, as shown in Table IV. These values indicate a reasonable agreement between the experimental and numerical responses, providing an acceptable representation the seismic behavior of the specimen.

TABLE III
Comparison response between experimental and numerical simulation for PSD1 test

	RMS		MAX	
	Specimen deformation x	Rest. force f_r	Specimen deformation x	Rest. force f_r
PSD1	7.35	1.30	43.25	6.05
Bilinear	8.90	1.65	43.75	6.13

TABLE IV
Comparison response between experimental and numerical simulation for PSD2 test

	RMS		MAX	
	Specimen deformation x	Rest. force f_r	Specimen deformation x	Rest. force f_r
PSD2	31.92	3.26	118.46	9.78
Bilinear	38.29	4.04	130.55	10.63

CONCLUSIONS

In this study, the application of PSD tests on the ABC-RU specimen was carried out. This test combines experimental data (such as restoring force) with a numerical analysis of the seismic response. A displacement control algorithm was used in the PSD test technique to accurately impose deformations on the specimen. To evaluate the reliability of this control algorithm, two tests (PSD1 and PSD2) were conducted on the ABC-RU specimen under two levels of axial load and ground motion. The experimental results were compared with those obtained from numerical simulations. Thus, the findings of this study lead to the following conclusions:

- The PSD tests were successfully conducted using the laboratory's equipment. This system was integrated with updated software and hardware, offering compatibility with the existing laboratory setup.
- The displacement control algorithm was evaluated in terms of RMS and MAX responses. The results showed that the displacement control worked properly, with a slight variation between the target displacements and the specimen deformation less than 0.3% for both RMS and MAX responses.

- A bilinear hysteresis model was adopted for the numerical simulation for both tests. The parameters of the bilinear model were determined by taking into account the stiffness slopes and the critical points found in the previous research work [15]. Consequently, a reasonable agreement was found between the responses in displacement and restoring force when comparing the numerical simulations with the results obtained from the experimental tests.

ACKNOWLEDGMENTS

The authors gratefully acknowledge the financial support from the Vice-rectorate for Research at The National University of Engineering, Peru. We would also like to express our sincere gratitude to the technical staff, colleagues, and the entire team at CISMID for their invaluable support during the structural testing phase of this research.

REFERENCES

[1] D. P. McCrumB, M. S. Williams, "An overview of seismic hybrid testing of engineering structures," *Engineering Structures*, vol. 118, pp. 240-261, 2016, doi: 10.1016/j.engstruct .2016.03.039

[2] P. Mortazavi, X. Huang, O. Kwon, and C. Christopoulos, "An overview of the University of Toronto (UT-SIM) Framework and its Application to the Performance Assessment of Structures," in Proc. 7th International Conference on Advances in Experimental Structural Engineering, Pavia, 2020. [Online]. Available: https://www.researchgate.net/publication/327405277_An_Overview_of_the_University_of_Toronto_Simulation_UT-SIM_Framework_and_its_Application_to_the_Performance_Assessment_of_Structures

[3] H. Kakoty, C. Kolay, S. Raj, and K. Kar, "Real-time hybrid simulation in the Pseudo-dynamic testing facility at the Indian Institute of Technology Kanpur," *Current Science*, vol. 125, no. 6, pp. 685-691, 2023, doi: 10.18520/cs/v125/i6/685-691

[4] C. Del Vecchio, M. Di Ludovico, A. Fiorillo, G. Verderame, A. Prota, G. Manfredi, and E. Cosenza, "The Pseudo-dynamic testing facility at UNINA: Preliminary Test on a RC Frame," Italian Concrete Conference, 2020, doi: 10.1007/978-3-031-37955-0_43

[5] S. Benedetto, A. Francavilla, M. Latour, G. Cavallaro, V. Piluso, and G. Rizzano, "Pseudo-dynamic testing of a full-scale two-storey steel building with RBS connections," *Engineering Structures*, vol. 212, pp. 110494, 2020, doi: 10.1016/j.engstruct .2020.110494

[6] H. Mishra, A. Igarashi, D. Ji, and H. Matsushima, "Pseudo-dynamic testing for seismic performance assessment of buildings with seismic isolation system using scrap tire rubber pad isolators," *Civil Engineering and Architecture*, vol. 8, no. 1, pp. 73-88, 2014, doi: 10.17265/1934-7359/2014.01.009

[7] K. Takanashi, and M. Nakashima, "Japanese activities on On-line testing", *Engineering Mechanics*, vol. 113, pp. 1014-1032, 1987, doi: 10.1061/(ASCE)0733-9399(1987)113:7(1014)

[8] H. Scaletti, V. Chariarse, C. Cuadra, and G. Cuadros, "Pseudo dynamic tests of confined masonry buildings," in Proc. 10th World Conference on Earthquake Engineering. Rotterdam, 1992. [Online]. Available: https://www.iitk.ac.in/nicee/wcee/article/10_vol6_3493.pdf

[9] G. Cuadros, "Estudio de modelos de albañilería confinada," Undergradute Thesis, Faculty of Civil Engineering, National University of Engineering, Lima, 1994. [Online]. Available: http://hdl.handle.net/20.500.14076/20219

[10] C. Chunga, "Desarrollo de software para el control de actuadores en línea en ensayos de estructuras a escala natural," Undergradute Thesis, Faculty of Civil Engineering, National University of Engineering, Lima, 2001. [Online]. Available: http://hdl.handle.net/20.500.14076/20357

[11] S. Mahin, and M. Williams, "Computer controlled seismic performance testing," in Proc. Second ASCE-EMD Specially Conference on Dynamic Response of Structures, Atlanta, 1981.

[12] P. S. Shing, and S. Mahin, "Pseudodynamic test method for seismic peformance evaluation: Theory and Implementation," College of Engineering at University of California, Technical Report, UCB/EERC-84/01, Jan. 1984. [Online]. Available: https://mechs.designsafe-ci.org/media/filer_public/92/82/9282cdb0-3886-4329-8fad-f9ea78563950/2_shing-mahin_pseudodynamictestmethod4seismicperformevaluation-theoryimplementation.pdf

[13] C. Zavala, "A study on substructuring hybrid simulation for flexible steel framed structures," PhD thesis, Graduate School of Engineering, University of Tokyo, Tokyo, 1994. [Online]. Available: https://dl.ndl.go.jp/pid/3115258/1/1

[14] R. Reyna, C. Zavala, E. Flores, J. Morales, L. Nuñez, Y. Taipicuri, and D. Velasquez, "Desarrollo de un prototipo de aislamiento sísmico de bajo costo (ABC) con disipación de energía mejorada," Vice-rectorate for Research at The National University of Engineering, Technical Report, FIC-FI-13-2020, 2021.

[15] R. Reyna, D. Velasquez, J. Chavez, and C. Zavala, "Experimental Study of Low-Cost Base Isolation prototype (ABC) with enhanced energy dissipation," in Proc. 18th World Conference on Earthquake Engineering, Milan, 2024.

[16] Ministerio de Vivienda, Construcción y Saneamiento. RM-030-2019-Vivienda Norma Técnica E.031 "Aislamiento Sísmico". [Online]. Available: https://www.gob.pe/institucion/sencico/informes-publicaciones/887225-normas-del-reglamento-nacional-de-edificaciones-rne

[17] C. Zavala, T. Kaminosono, "Construction Monitoring and Improvement Techniques for Masonry Housing," CISMID-FIC-National University of Engineering, Technical report, 2003.

[18] Ministerio de Vivienda, Construcción y Saneamiento. RM-355-2018-Vivienda Norma Técnica E.030 "Diseño Sismorresistente". [Online]. Available: https://www.gob.pe/institucion/sencico/informes-publicaciones/887225-normas-del-reglamento-nacional-de-edificaciones-rne